# Supplementary Information

**Red emitting ionic fluorophores: Anion dependent tunable fluorescence, chlorinated solvent sensing, white light emission and latent fingerprinting**

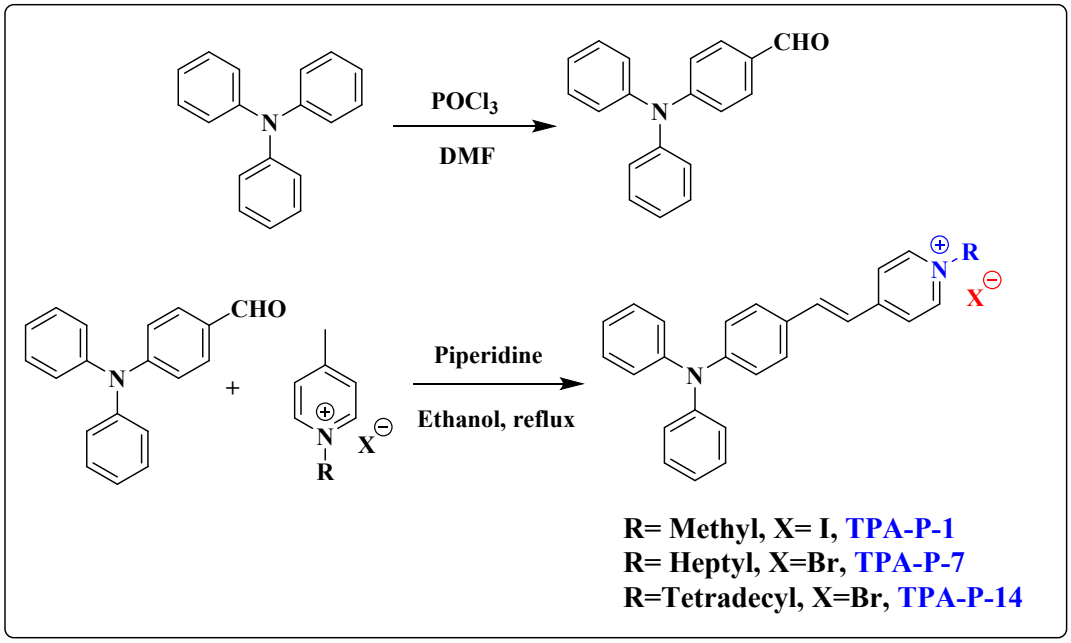


**Scheme S1.** Synthesis of (E)-4-(4-(diphenylamino)styryl)-1-alkylpyridin-1-ium salts

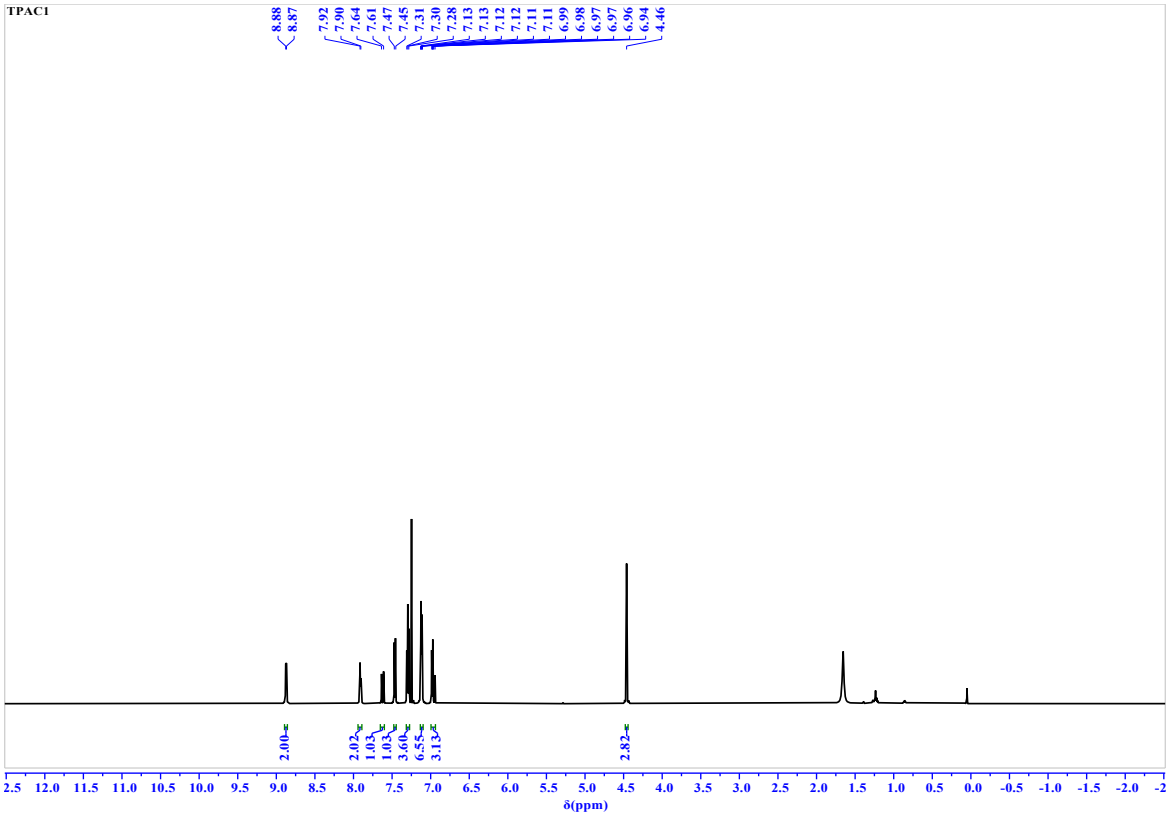


**$^{1}$H NMR spectra of TPA-P-1**

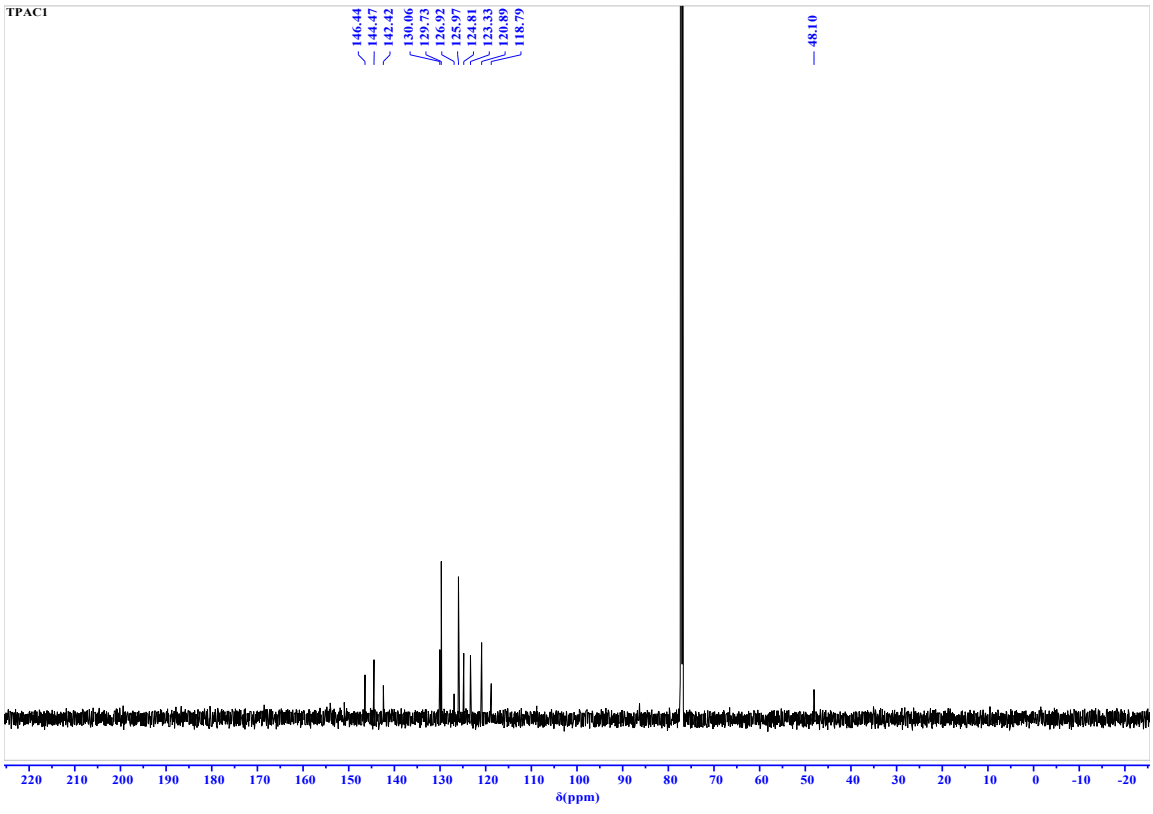


**$^{13}$C NMR spectra of TPA-P-1**

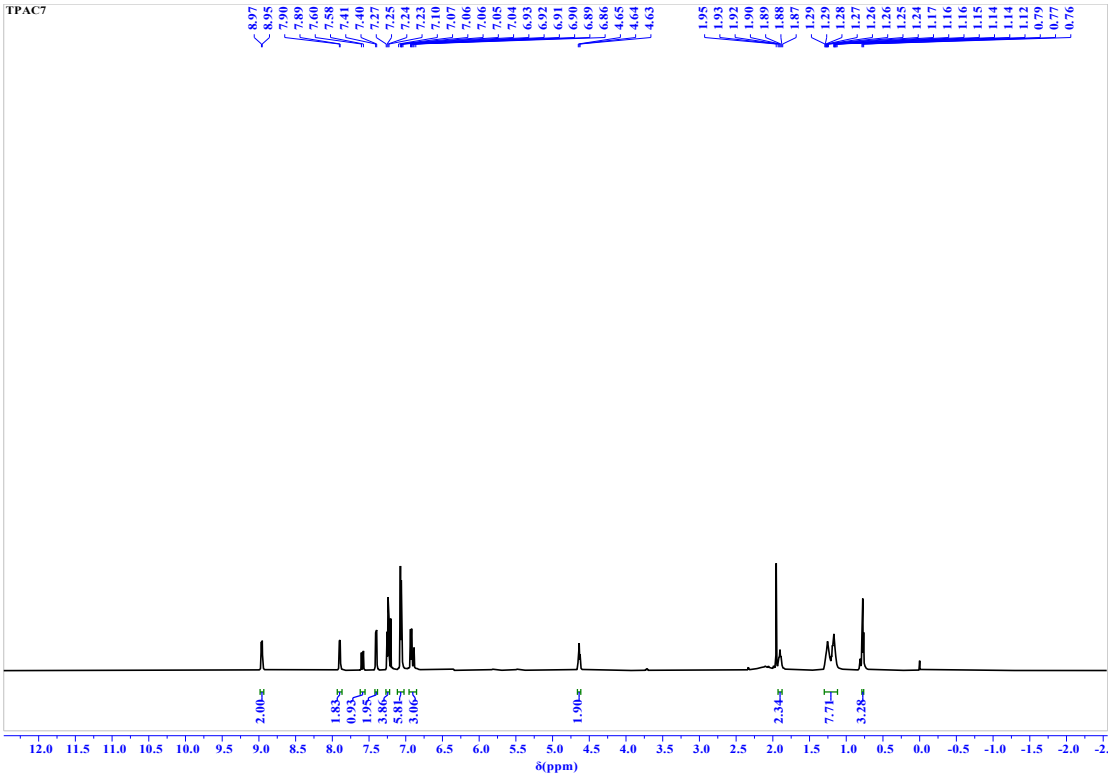


**$^{1}$H NMR spectra of TPA-P-7**

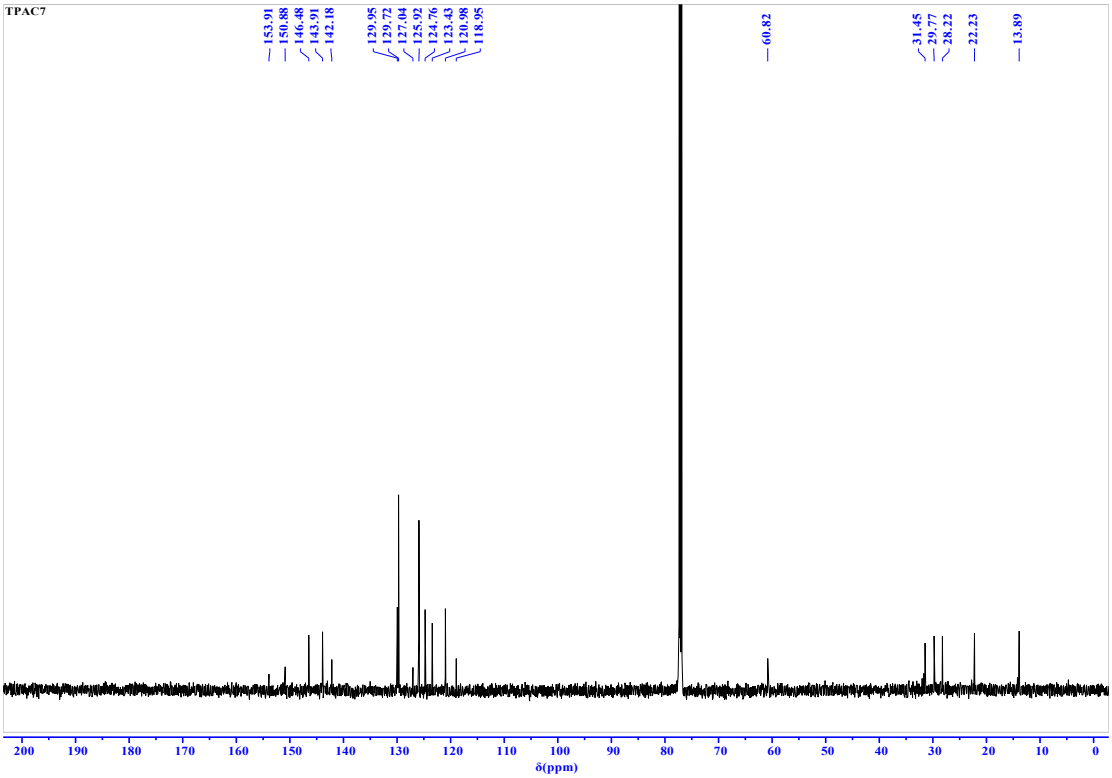


**$^{13}$C NMR spectra of TPA-P-7**

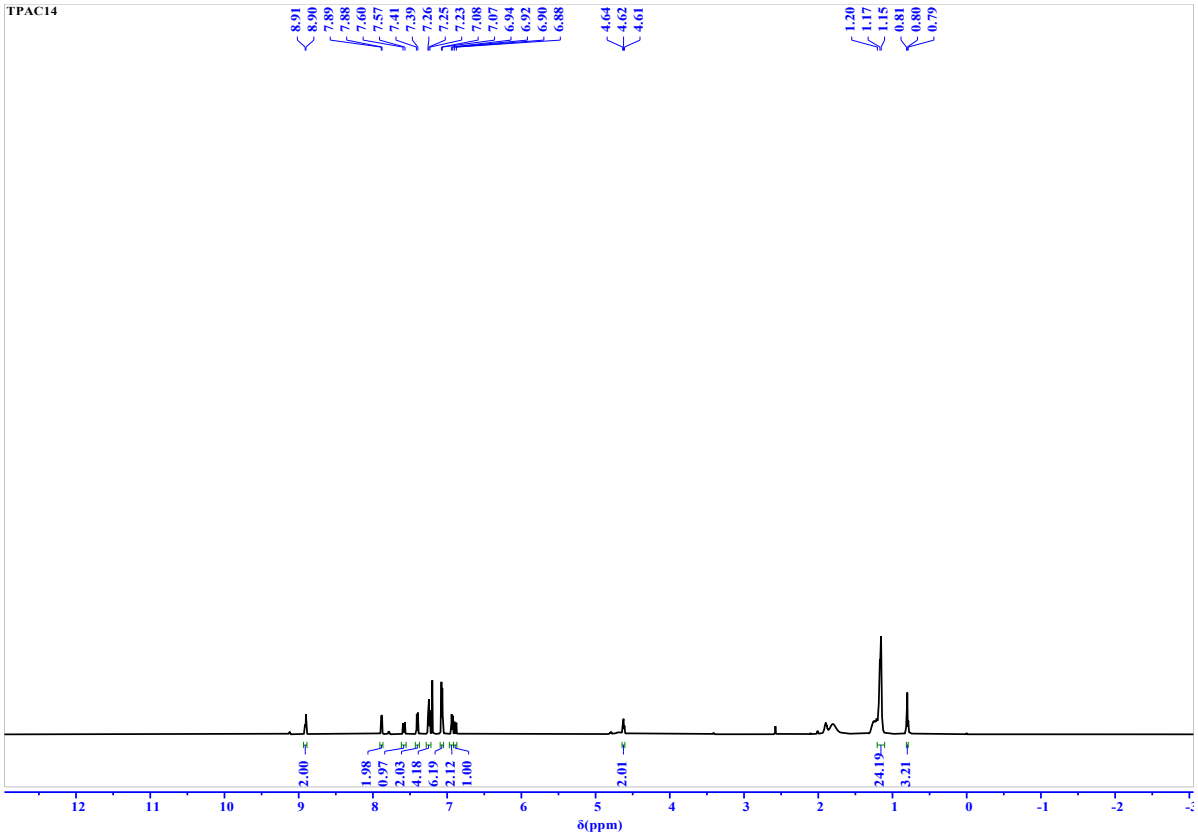


**$^{1}$H NMR spectra of TPA-P-14**

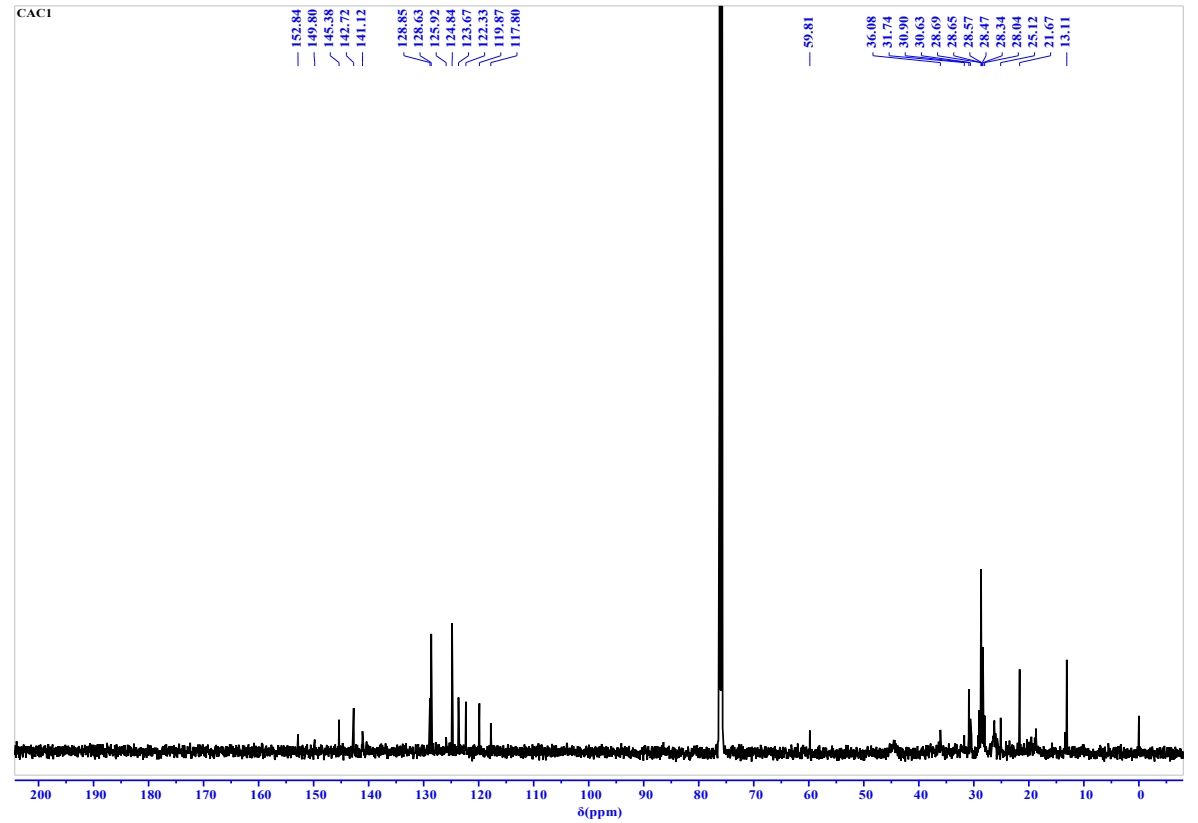


**$^{13}$C NMR spectra of TPA-P-14**

Table S1. Crystallographic data of **TPA-P-1** I (CCDC No. 2353725).

| | | |
|---|---|---|
| Empirical formula | C26 H23 I N2 | |
| Formula weight | 490.36 | |
| Temperature | 220(2) K | |
| Wavelength | 0.700 Å | |
| Crystal system | Triclinic | |
| Space group | P-1 | |
| Unit cell dimensions | a = 11.679(2) Å | a = 76.14(3)° |
| | b = 17.758(4) Å | b = 82.02(3)° |
| | c = 23.966(5) Å | g = 71.88(3)° |
| Volume | 4575.3(19) $Å^3$ | |
| Z | 8 | |
| Density (calculated) | 1.424 $Mg/m^3$ | |
| Absorption coefficient | 1.340 $mm^{-1}$ | |
| F(000) | 1968 | |
| Crystal size | 0.039 x 0.011 x 0.009 $mm^3$ | |
| Theta range for data collection | 1.811 to 24.999°. | |
| Index ranges | -14<=h<=14, -21<=k<=21, -28<=l<=28 | |
| Reflections collected | 32943 | |
| Independent reflections | 16669 [R(int) = 0.0392] | |
| Completeness to theta = 24.835° | 98.8 % | |
| Absorption correction | Empirical | |
| Max. and min. transmission | 1.000 and 0.645 | |
| Refinement method | Full-matrix least-squares on $F^2$ | |
| Data / restraints / parameters | 16669 / 20 / 1088 | |
| Goodness-of-fit on $F^2$ | 0.996 | |
| Final R indices [I>2sigma(I)] | R1 = 0.0666, wR2 = 0.2003 | |
| R indices (all data) | R1 = 0.0965, wR2 = 0.2192 | |
| Extinction coefficient | 0.0013(2) | |
| Largest diff. peak and hole | 1.156 and -0.963 $e \cdot Å^{-3}$ | |

Table S2. Crystallographic data of **TPA-P-1** I OTs (CCDC No. 2353726).

| | | |
|---|---|---|
| Empirical formula | C59 H53 I N4 O3 S | |
| Formula weight | 1025.01 | |
| Temperature | 220(2) K | |
| Wavelength | 0.630 Å | |
| Crystal system | Triclinic | |
| Space group | P-1 | |
| Unit cell dimensions | a = 9.3240(19) Å | a= 95.64(3)°. |
| | b = 10.641(2) Å | b= 98.83(3)°. |
| | c = 26.345(5) Å | g = 99.25(3)°. |
| Volume | 2529.0(9) $Å^3$ | |
| Z | 2 | |
| Density (calculated) | 1.346 $Mg/m^3$ | |
| Absorption coefficient | 0.520 $mm^{-1}$ | |
| F(000) | 1056 | |
| Crystal size | 0.075 x 0.011 x 0.009 $mm^3$ | |
| Theta range for data collection | 1.398 to 25.000°. | |
| Index ranges | -12<=h<=12, -14<=k<=14, -35<=l<=35 | |
| Reflections collected | 25033 | |
| Independent reflections | 12642 [R(int) = 0.0227] | |
| Completeness to theta = 22.210° | 99.1 % | |
| Absorption correction | Empirical | |
| Max. and min. transmission | 1.000 and 0.819 | |
| Refinement method | Full-matrix least-squares on $F^2$ | |
| Data / restraints / parameters | 12642 / 372 / 635 | |
| Goodness-of-fit on $F^2$ | 1.097 | |
| Final R indices [I>2sigma(I)] | R1 = 0.0703, wR2 = 0.2030 | |
| R indices (all data) | R1 = 0.1041, wR2 = 0.2215 | |
| Extinction coefficient | n/a | |
| Largest diff. peak and hole | 1.402 and -1.086 $e.Å^{-3}$ | |

Table S3. Crystallographic data of **TPA-P-1** (CCDC No. 2353727).

| | | |
|---|---|---|
| Identification code | SPA853 | |
| Empirical formula | C26 H23 Cl N2 O4 | |
| Formula weight | 462.91 | |
| Temperature | 220(2) K | |
| Wavelength | 0.630 Å | |
| Crystal system | Monoclinic | |
| Space group | $P2_1/c$ | |
| Unit cell dimensions | a = 11.327(2) Å | a= 90°. |
| | b = 20.280(4) Å | b= 109.77(3)°. |
| | c = 10.453(2) Å | g = 90°. |
| Volume | 2259.7(9) $Å^3$ | |
| Z | 4 | |
| Density (calculated) | 1.361 $Mg/m^3$ | |
| Absorption coefficient | 0.150 $mm^{-1}$ | |
| F(000) | 968 | |
| Crystal size | 0.045 x 0.027 x 0.012 $mm^3$ | |
| Theta range for data collection | 1.693 to 24.997°. | |
| Index ranges | -15<=h<=15, -27<=k<=27, -13<=l<=12 | |
| Reflections collected | 21162 | |
| Independent reflections | 5403 [R(int) = 0.0411] | |
| Completeness to theta = 22.210° | 95.6 % | |
| Absorption correction | Empirical | |
| Max. and min. transmission | 1.000 and 0.812 | |
| Refinement method | Full-matrix least-squares on $F^2$ | |
| Data / restraints / parameters | 5403 / 0 / 299 | |
| Goodness-of-fit on $F^2$ | 1.073 | |
| Final R indices [I>2sigma(I)] | R1 = 0.0573, wR2 = 0.1596 | |
| R indices (all data) | R1 = 0.0831, wR2 = 0.1710 | |
| Extinction coefficient | n/a | |
| Largest diff. peak and hole | 1.015 and -0.407 $e.Å^{-3}$ | |

Table S4. Crystallographic data of **TPA-P-14** $ClO_4$ (CCDC No. 2353728).

| | | |
|---|---|---|
| Empirical formula | C78 H100 Cl2 N4 O9 | |
| Formula weight | 1308.51 | |
| Temperature | 220(2) K | |
| Wavelength | 0.630 Å | |
| Crystal system | Triclinic | |
| Space group | P-1 | |
| Unit cell dimensions | a = 8.8910(18) Å | a= 93.24(3)°. |
| | b = 11.629(2) Å | b= 91.19(3)°. |
| | c = 36.418(7) Å | g = 102.33(3)°. |
| Volume | 3670.5(13) $Å^3$ | |
| Z | 2 | |
| Density (calculated) | 1.184 $Mg/m^3$ | |
| Absorption coefficient | 0.108 $mm^{-1}$ | |
| F(000) | 1404 | |
| Crystal size | 0.079 x 0.069 x 0.022 $mm^3$ | |
| Theta range for data collection | 1.490 to 25.000°. | |
| Index ranges | -11<=h<=11, -15<=k<=15, -48<=l<=48 | |
| Reflections collected | 34604 | |
| Independent reflections | 17488 [R(int) = 0.0213] | |
| Completeness to theta = 22.210° | 95.2 % | |
| Absorption correction | Empirical | |
| Max. and min. transmission | 1.000 and 0.816 | |
| Refinement method | Full-matrix least-squares on $F^2$ | |
| Data / restraints / parameters | 17488 / 27 / 845 | |
| Goodness-of-fit on $F^2$ | 1.201 | |
| Final R indices [I>2sigma(I)] | R1 = 0.1016, wR2 = 0.3220 | |
| R indices (all data) | R1 = 0.1500, wR2 = 0.3580 | |
| Extinction coefficient | 0.0033(16) | |
| Largest diff. peak and hole | 1.085 and -0.782 $e.Å^{-3}$ | |

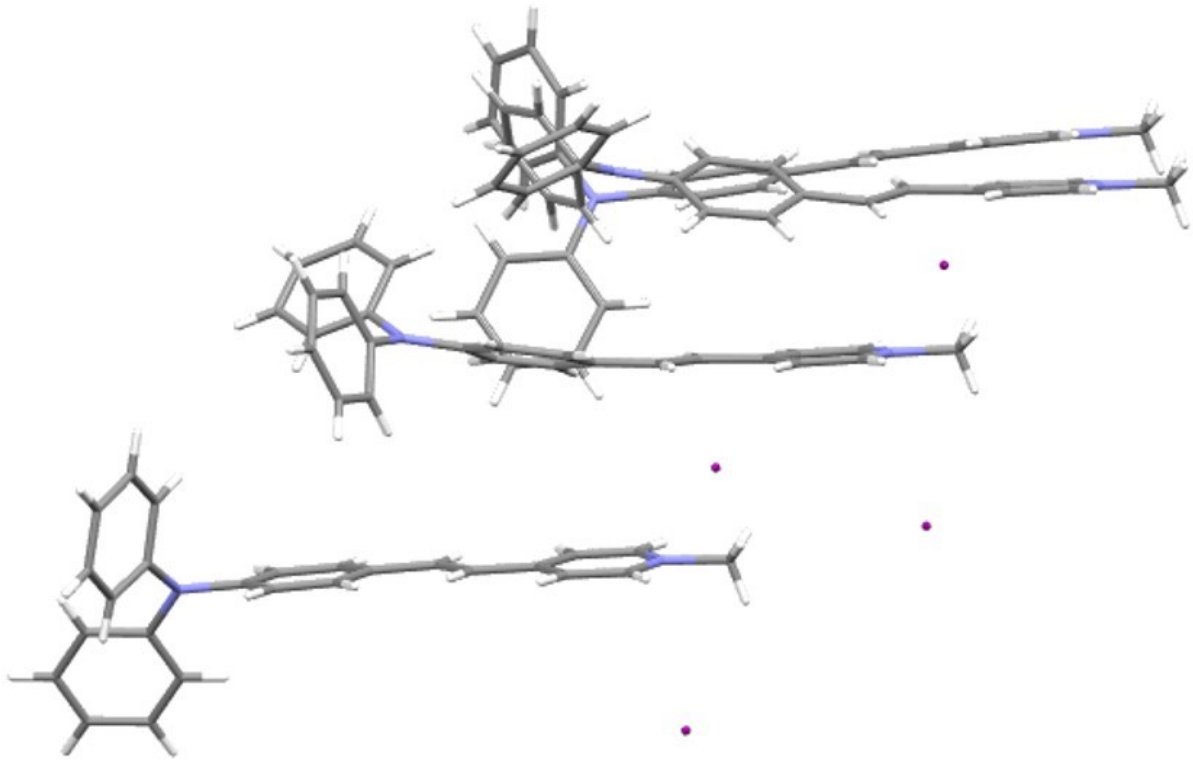

Fig. S1. Molecular structure of **TPA-P-1** I in the asymmetric unit.

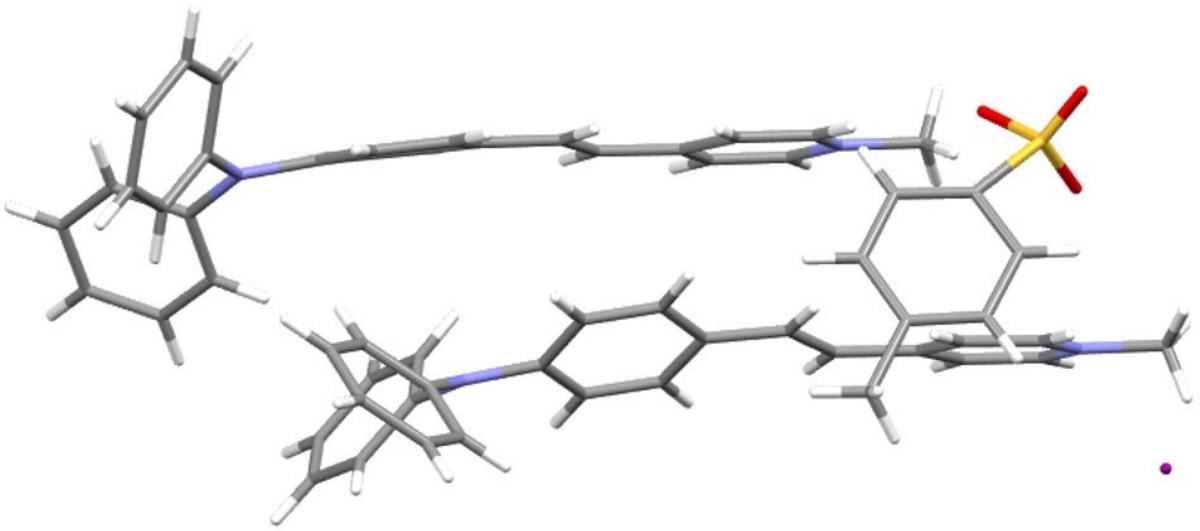

Fig. S2. Molecular structure of **TPA-P-1** OTs in the asymmetric unit.

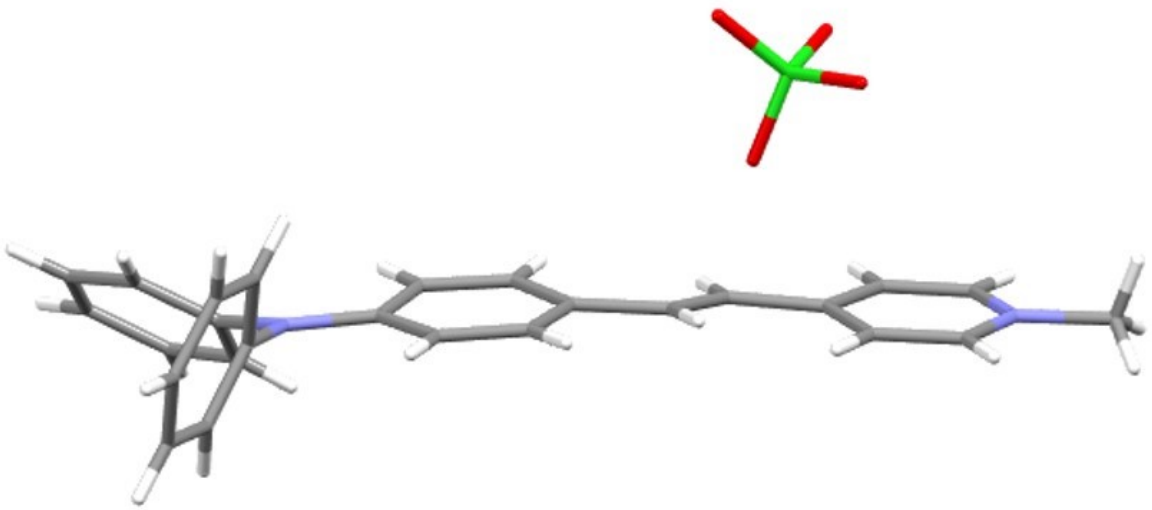

Fig. S3. Molecular structure of **TPA-P-1** $ClO_4$ in the asymmetric unit.

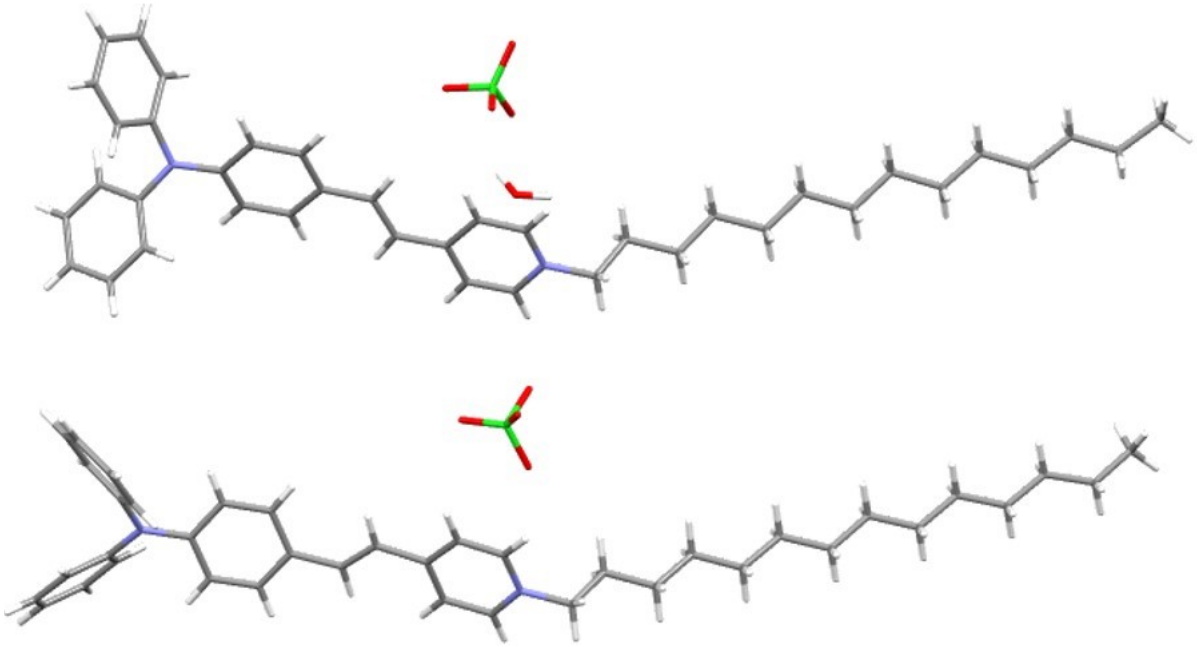

Fig. S4. Molecular structure of **TPA-P-14** $ClO_4$ in the asymmetric unit.

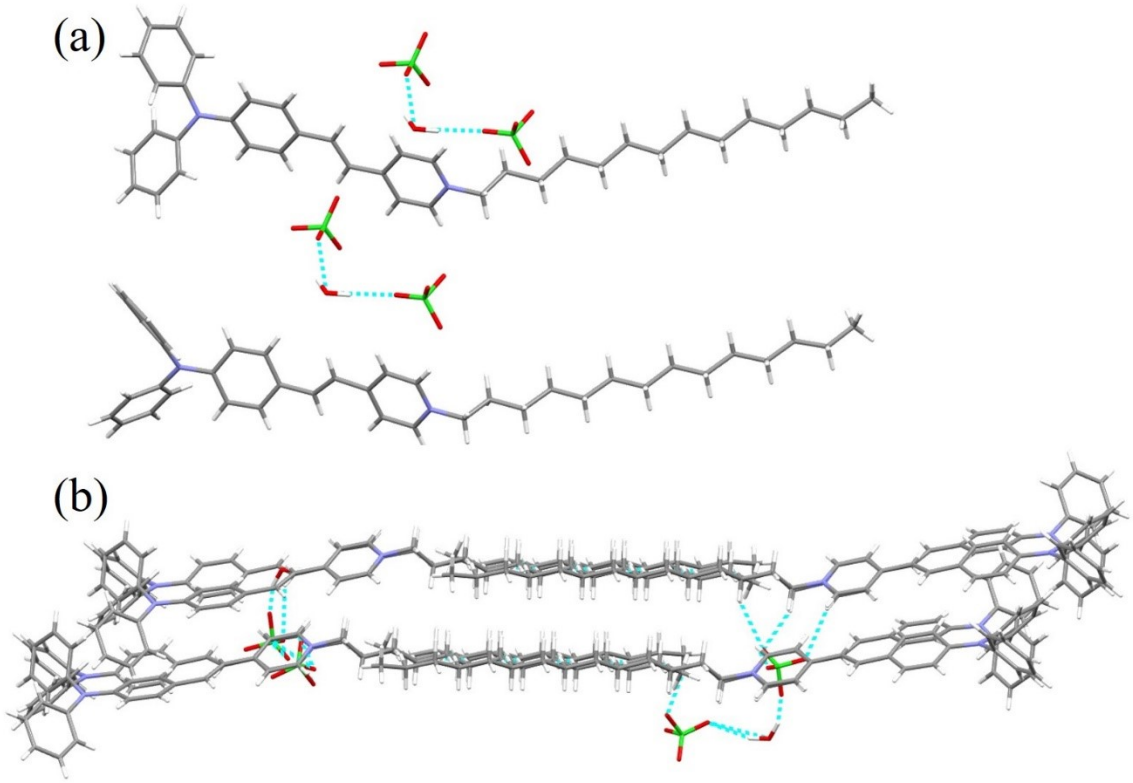


Fig. S5. Intermolecular interactions in the crystal lattice of **TPA-P-14** $ClO_4$. (a) The H-bonding distance ($d_{D\text{-}H\ldots A}$) between water and perchlorate is ranged between 2.938-2.997 Å. (b) The H-bonding distance ($d_{D\text{-}H\ldots A}$) between pyridyl hydrogen and perchlorate is ranged between 2.913-3.090 Å.

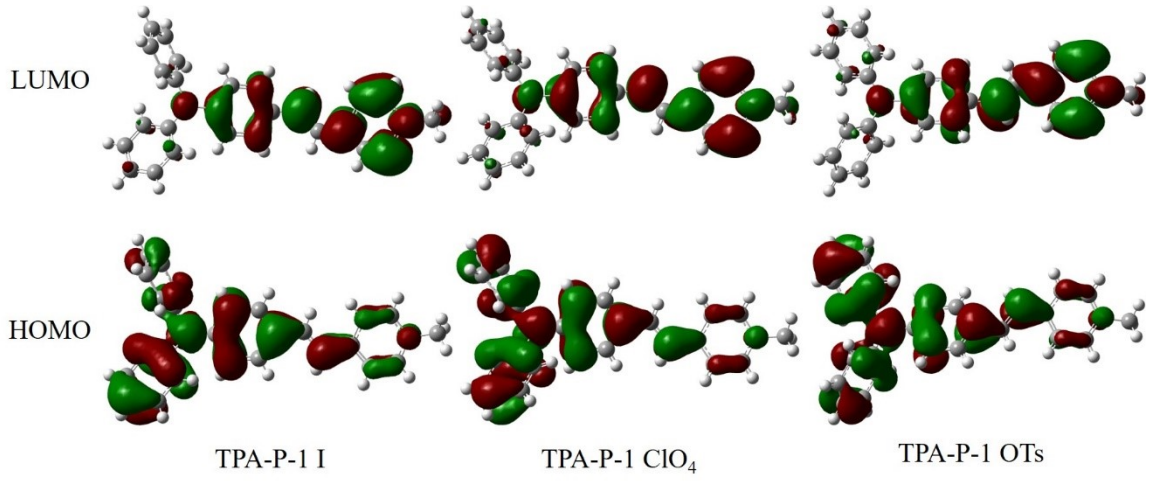


Fig. S6. HOMO-LUMO of **TPA-P-1** derived from different crystals.

Table S5. Calculated optical band of **TPA-P-1** structure obtained from the crystal structure.

| Compound | HOMO | LUMO | band gap(eV) |
|---|---|---|---|
| TPA-P-1 I | -7.61 | -5.61 | 2.00 |
| TPA-P-1 $ClO_4$ | -7.60 | -5.61 | 1.99 |
| TPA-P-1 OTs | -7.60 | -5.62 | 1.98 |

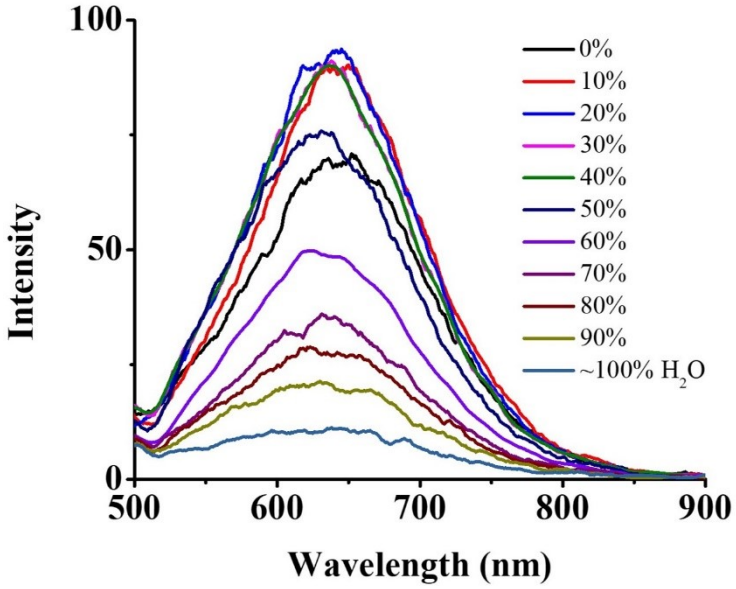


Fig. S7. AIE of **TPA-P-1** I in DMSO: water mixture.

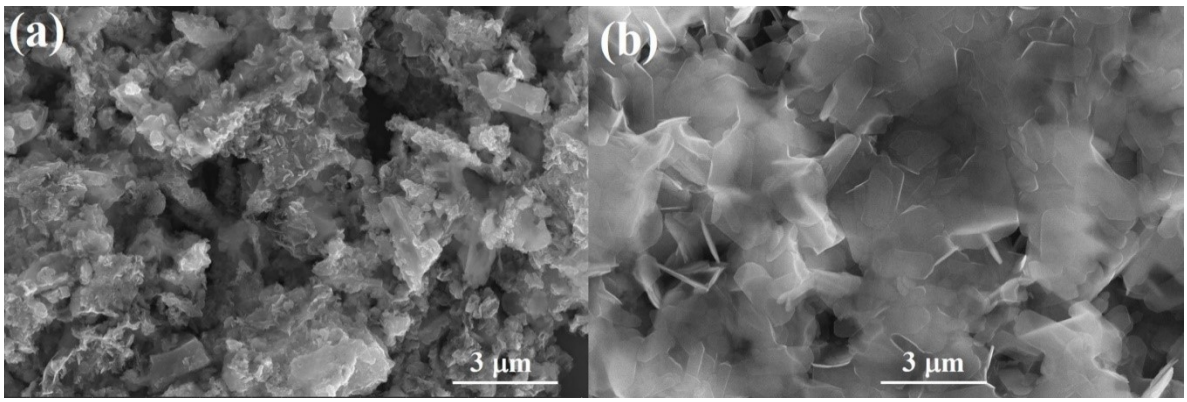


Fig. S8. FE-SEM images of (a) **TPA-P-7** and (b) **TPA-P-14** aggregates formed at ≈100% water.

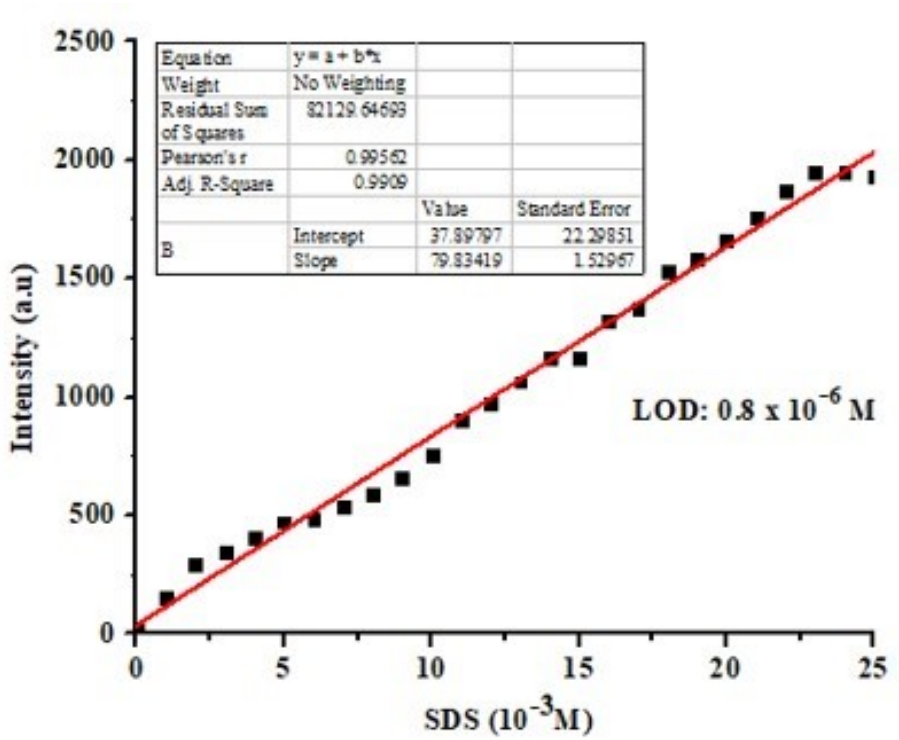


Fig. S9. Concentration dependent fluorescence of **TPA-P-1** I with SDS and LOD analysis.

Table S6. Percent (%) molecular orbital contribution of the HOMO and LUMO of the **TPA-P-1** at the B3LYP/6-31+G(d,p) Level

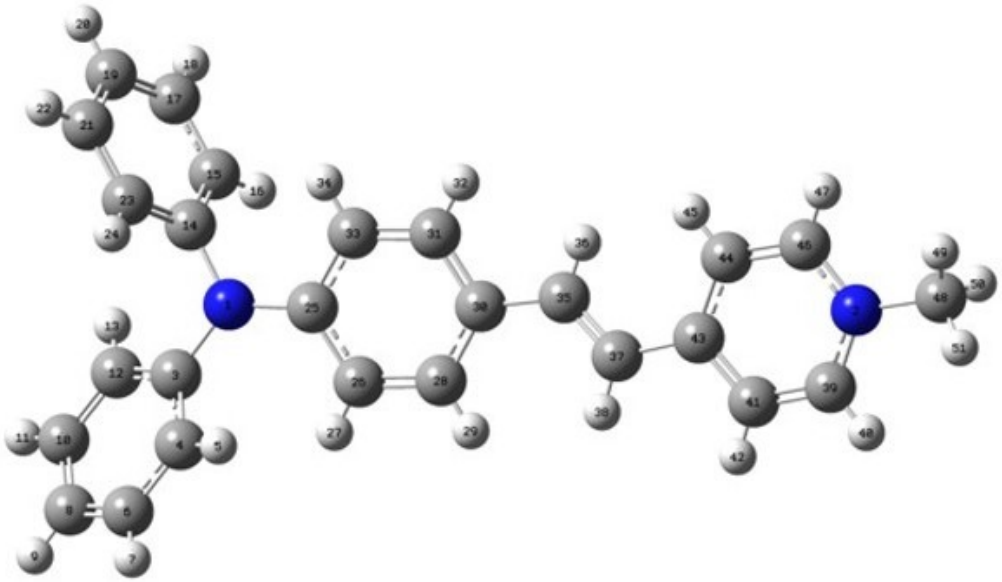

| | E(eV) | Band gap (eV) | Fragment 1 (atom 1 to atom 34) % | Fragment 2 (atom 35 to atom 51) % |
|---|---|---|---|---|

| | | | | |
|---|---|---|---|---|
| HOMO | -7.61 | 2.00 | 80 | 20 |
| LUMO | -6.61 | | 39 | 61 |

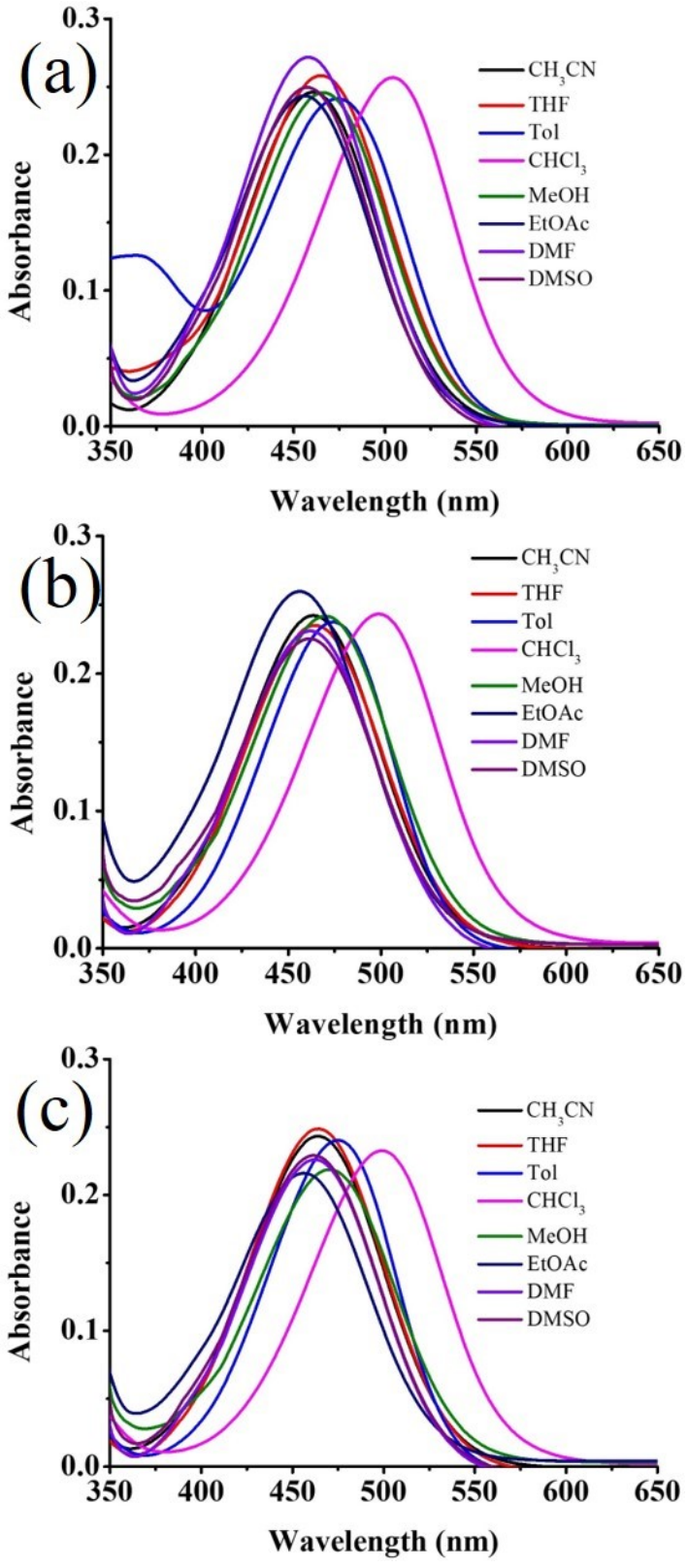

Fig. S10. Absorption spectra of (a) **TPA-P-1** I, (b) **TPA-P-7** Br and (c) **TPA-P-14** Br in different solvents.

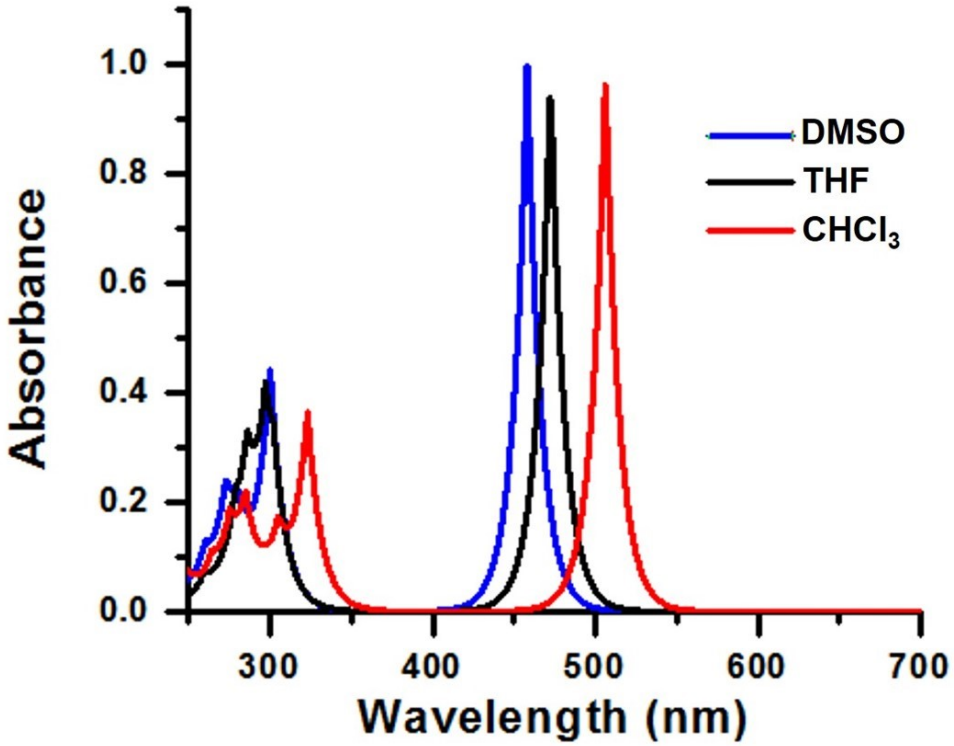


Fig. S11. Simulated absorption spectra of **TPA-P-1** in $CHCl_3$, THF and DMSO.

Table S7. Comparison of simulated absorption and experimental absorption of **TPA-P-1**.

| **Solvent** | **Experimental ($\lambda_{abs}$) nm** | **Theoretical ($\lambda_{abs}$) nm** |
|---|---|---|
| DMSO | 456 | 458 |
| THF | 467 | 473 |
| $CHCl_3$ | 508 | 516 |

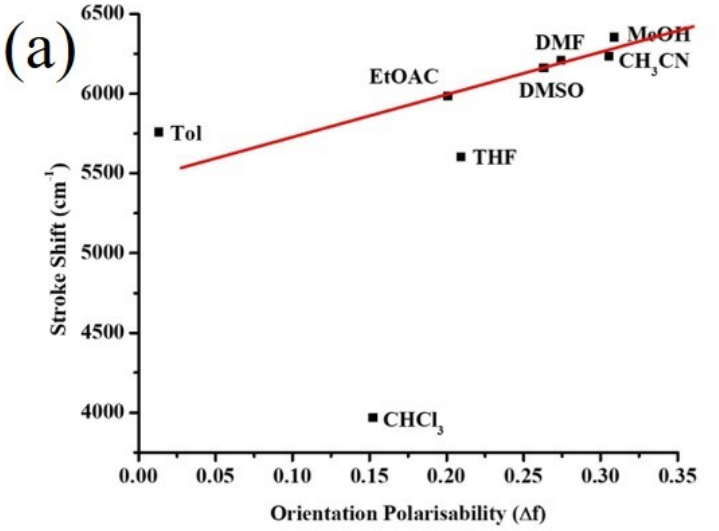
(a)
Stroke Shift (cm-1)
Orientation Polarisability (Δf)
Tol
EtOAC
DMF
MeOH
CH3CN
DMSO
THF
CHCl3

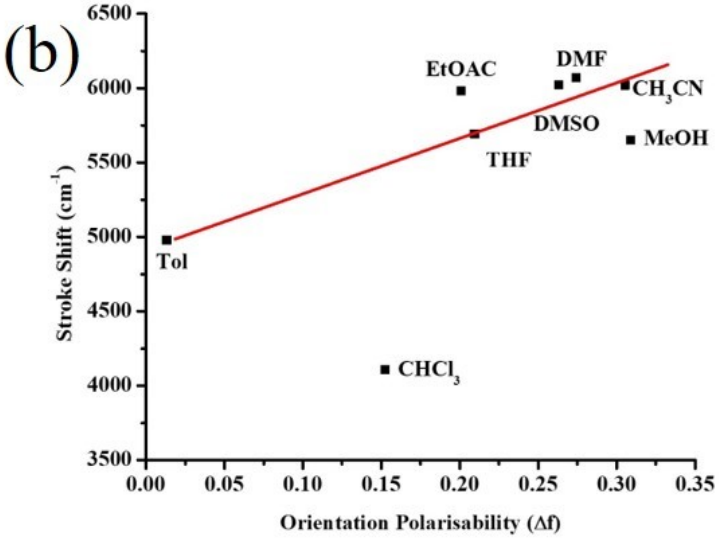
(b)
Stroke Shift (cm-1)
Orientation Polarisability (Δf)
Tol
EtOAC
DMF
CH3CN
DMSO
MeOH
THF
CHCl3

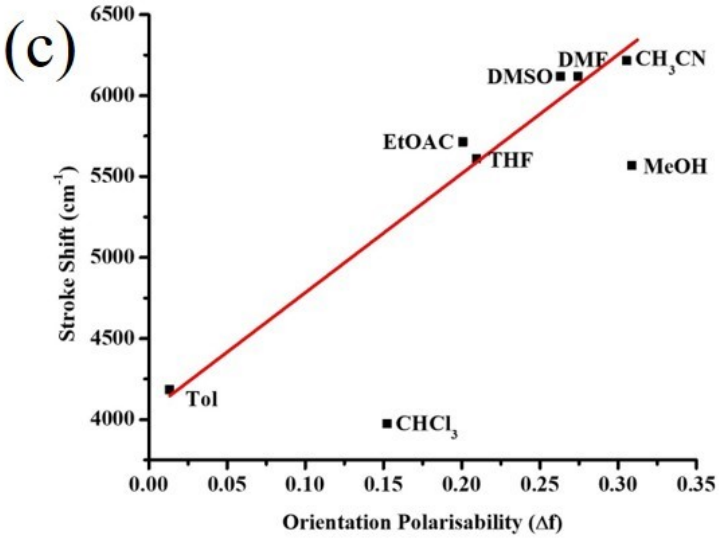
(c)
Stroke Shift (cm-1)
Orientation Polarisability (Δf)
Tol
DMSO
DMF
CH3CN
EtOAC
THF
MeOH
CHCl3

Fig. S12. Linear correlation of the orientation polarization (*f*) of solvent with Stokes shift ($\nu_a$ - $\nu_f$) for (a) **TPA-P-1**, (b) **TPA-P-7** and (c) **TPA-P-14**.

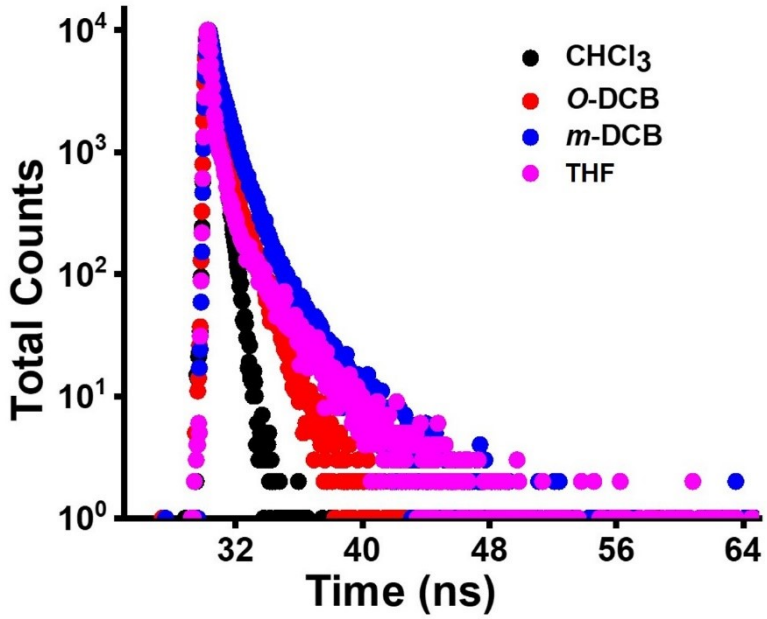


Fig. S13. Excited state decay profiles of **TPA-P-1** in $CHCl_3$, THF and DMSO.

| **Solvent** | **$B_1$** | **$B_2$** | $\tau_1$ | $\tau_2$ | **<τ> (ns)** | $\chi^2$ |
|---|---|---|---|---|---|---|
| $CHCl_3$ | 0.65 | 0.35 | 0.079 | 0.383 | 0.298 | 0.78 |
| *O*-DCB | 0.86 | 0.14 | 0.226 | 1.012 | 0.557 | 0.85 |
| *m*-DCB | 0.83 | 0.17 | 0.525 | 1.559 | 0.916 | 1.03 |
| THF | 0.98 | 0.02 | 0.172 | 1.838 | 0.470 | 0.97 |

Table S8. Shows the $\chi^2$ value and fluorescence life time decay of TPA-P-1 in $CHCl_3$, *O*-DCB, *m*-DCB, THF respectively in solution state, $B_1$, $B_2$ are relative individual component contributions to $\tau_1, \tau_2$ $< \tau >$ (ns) is the average lifetime from multiple decay profiles.

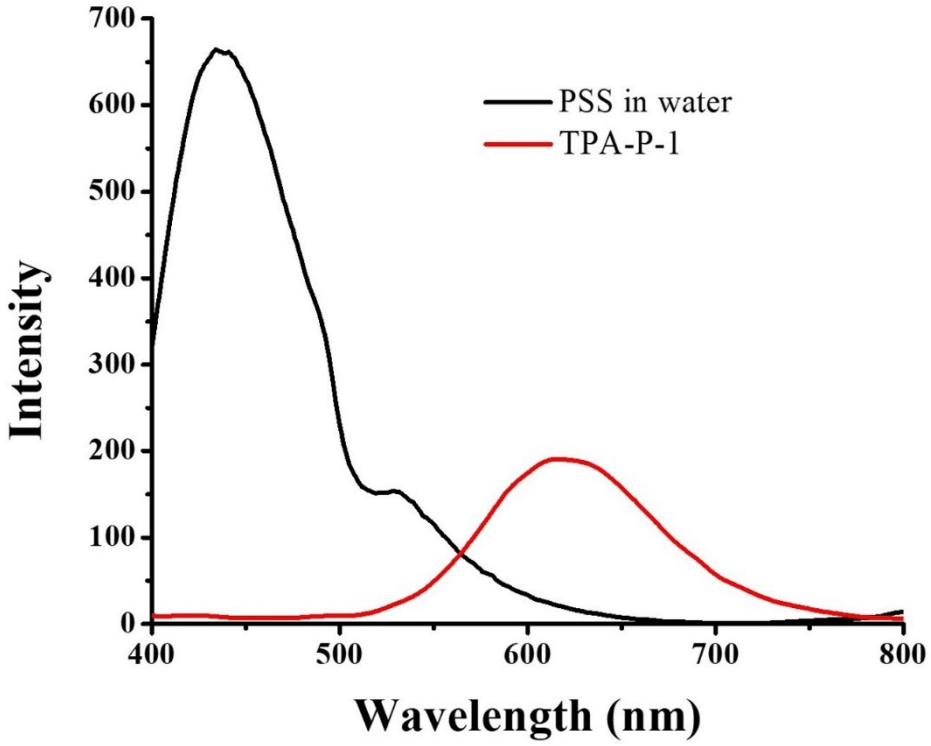


Fig. S14. Fluorescence spectra of PSS and **TPA-P-1** I in water.

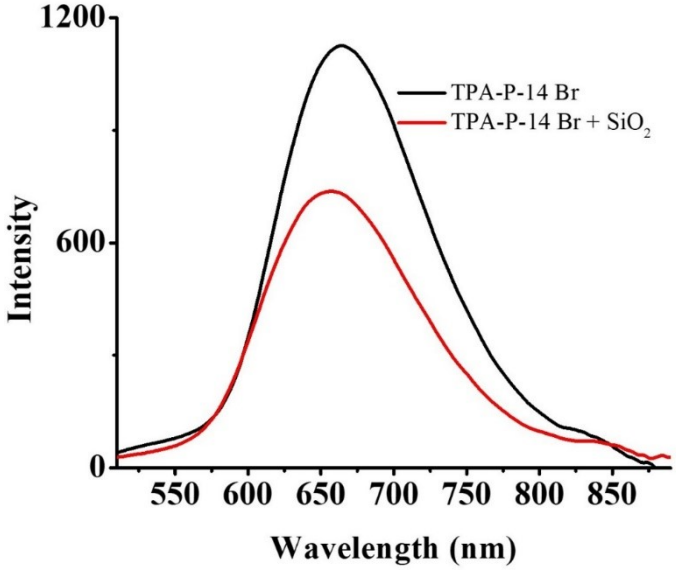


Fig. S15. Fluorescence spectra of **TPA-P-1** I before and after integrating with $SiO_2$.

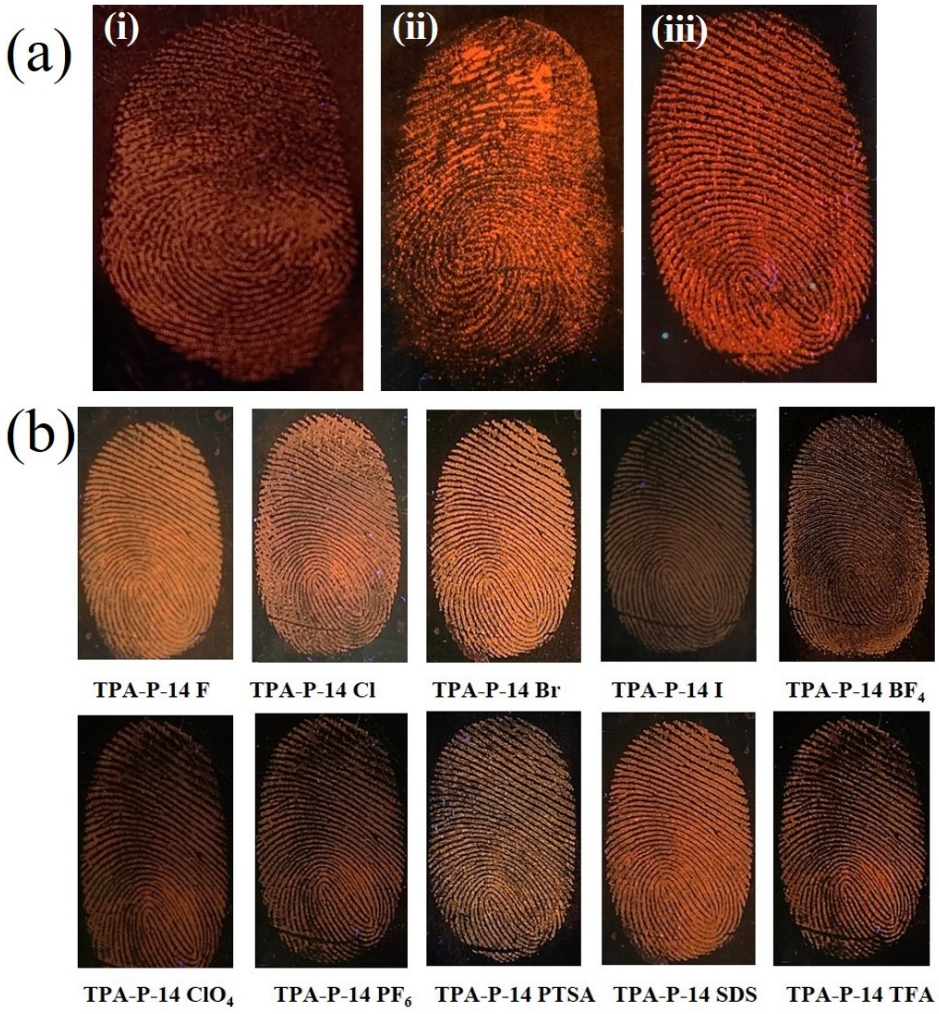


Fig. S16. LFPs imaging using (a) **TPA-P-1** I (i), **TPA-P-7** Br (ii) and **TPA-P-14** Br (iii) and (b) **TPA-P-14** with different anions. Fig. S16a (iii) and Fig. 6c (i) are same images. The duplicate image of **TPA-P-14** Br was used in Figure S16a (iii) to compare the image quality with the one obtained using **TPA-P-1** I and **TPA-P-7** Br.